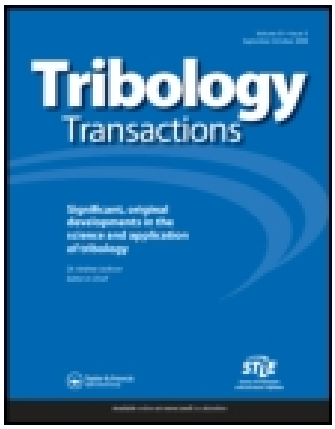

Tribology Transactions
Publication details, including instructions for authors and subscription information:
http://www.tandfonline.com/loi/utrb20

The Lubrication Effect of Micro-Pits on Parallel Sliding Faces of SiC in Water

Xiaolei Wang [a] , Koji Kato [a] & Koshi Adachi [a]
[a] Tohoku University, Laboratory of Tribology, School of Mechanical Engineering , Sendai, 980-8579, Japan
Published online: 25 Mar 2008.

To cite this article: Xiaolei Wang , Koji Kato & Koshi Adachi (2002) The Lubrication Effect of Micro-Pits on Parallel Sliding Faces of SiC in Water, Tribology Transactions, 45:3, 294-301, DOI: 10.1080/10402000208982552

To link to this article: http://dx.doi.org/10.1080/10402000208982552

Vol. 45 (2002), 3, 294-301
TRIBOLOGY TRANSACTIONS

The Lubrication Effect of Micro-Pits on Parallel Sliding Faces of SiC in Water©

XIAOLEI WANG, KOJI KATO and KOSHI ADACHI
Tohoku University
Laboratory of Tribology
School of Mechanical Engineering
Sendai, 980-8579, Japan

Silicon carbide is regarded as a promising material for sliding bearings and mechanical seals working in water. In order to improve its load carrying capacity (or anti-seizure ability) in water, micro-pits were formed on one of the contact surfaces by ion reaction etching. The effect of micro-pits on the critical load for the transition from EHL to mixed lubrication was studied experimentally in the cases of bearing type contact (with relatively rich water supply) and seal type contact (with relatively poor water supply). In order to understand the mechanisms of the lubrication effect of micro-pits, the experimental results obtained from bearing type contact and seal type contact were compared, and a theoretical analysis was carried out.

KEY WORDS

Surface Texturing; Ceramic; Water; Load Carrying Capacity

INTRODUCTION

Saving energy and reducing the amount of pollution released to the environment have increasingly become the most important concepts in machine design. Instead of metal and oil, silicon carbide is considered as a promising material for sliding bearings and mechanical seals working in water due to its excellent tribological properties such as anti-wear, anti-seizure, anti-corrosion, and in particular, very low friction while it slides against the same material in water (Nau, (1997), Wong, et al., (1998)). The reason for low friction is that a kind of tribo-chemical reaction occurs. Consequently, the reaction product SiO_2 dissolves in water as silicic acid, which is recognized to act as a lubricant, and the contact surfaces become very smooth due to tribo-chemical wear (Wong, et al., (1998), Sugita, et al., (1984), Ishigaki, et al., (1988)).

However, seizure still happens due to instantaneous overload on the contact surface. Furthermore, the demands for higher pressure and speed of bearing and seal system have a steep rise in recent years. Therefore, to improve the load carrying capacity of sliding contact should be our permanent research subject for the reliability of sliding bearings and mechanical seals.

For the hydrodynamic pressure generated between parallel sliding surfaces, several mechanisms were summarized in (Ludwig, et al., (1978), Lebeck, (1987)). Surface roughness is recognized as an important role and then this discovery brought about the method of surface texturing for improving the load carrying capacity or anti-seizure ability of sliding contact.

Research on the lubrication of surface textures has been carried out for a long time. So far, many types of surface texture including micro-islands (Hamilton, et al., (1966), Anno, et al. (1968)), spiral grooves (Lai, (1994)) and micro-pits (Etsion, et al., (1996),

Presented at the 57th Annual Meeting
Houston, Texas
May 19-23, 2002
Final manuscript approved April 29, 2002
Review led by Tom Lai

NOMENCLATURE

a	$= h_1/h_2$
d	= diameter of the pit, μm
h	= pit depth, μm
h_1, h_2	= film thickness, μm
L, L_1	= step bearing length coordinate, μm
Pm	= maxim hydrodynamic pressure, Pa
r	= pit area ratio
s	$= L_1/L$
U	= average circumferential velocity, m/s
W	= load, N
$\bar{W}$	= dimensionless load
Wc	= the critical load for the transition from hydrodynamic to mixed lubrication, N
Wc_0	= the critical load of untextured specimen at a rotational speed of 800 rpm, N
η	= viscosity of lubricant, Pa•s
μ	= friction coefficien

TABLE 1—PHYSICAL PROPERTIES OF THE SiC USED IN THIS EXPERIMENT

Density	3100 kg/m^3
Bending strength	470 MPa
Vickers hardness	2800
Coefficient of thermal expansion	4.02x10^{-6}/K
Thermal conductivity	125.6 W/m•K

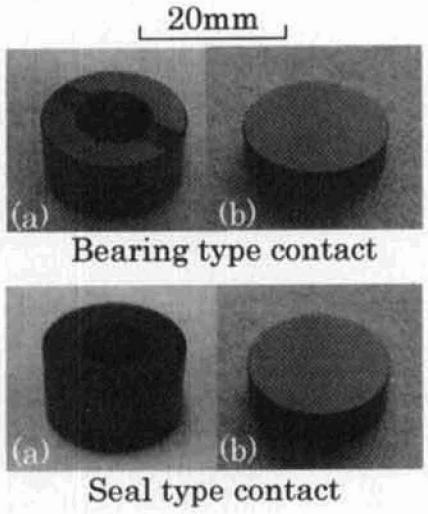

Fig. 1—Photographs of the specimens.
(a) cylinder
(b) disk

Halperin, et al., (1997), Geiger, et al., (1998), Etsion, et al., (1999), Tejima, et al., (1999), Wang, et al., (2000), (2001)), were studied. Various manufacturing techniques are utilized to produce textures on the contact surfaces. Photo etching is a traditional method which deals with the surface of copper. Laser is efficient and convenient for metals. Erosion is an effective technique for hard materials.

It was reported that proper textures are able to increase lubrication film stiffness and PV factor at seizure inception (Halperin, et al., (1997)), to decrease the minimum friction coefficient (Tejima, et al., (1999)), to expand the low friction region (Wang, et al., (2000)) and extend the safe running time after lubricant supply is stopped (Wang, et al., (2001)).

For the most researches concerned, the effect of surface texture is emphasized as a way to generate additional hydrodynamic pressure (Hamilton, et al., (1966), Anno, et al., (1968), Etsion, et al., (1996)). This is due to an asymmetric hydrodynamic pressure distribution over the wavy surfaces. Usually, the pressure increase in the converging film regions is much larger than the pressure drop in diverging film regions where cavitation occurs.

The words "secondary lubrication effect" is used for describing the pit effect in the case of intimate contact such as metal

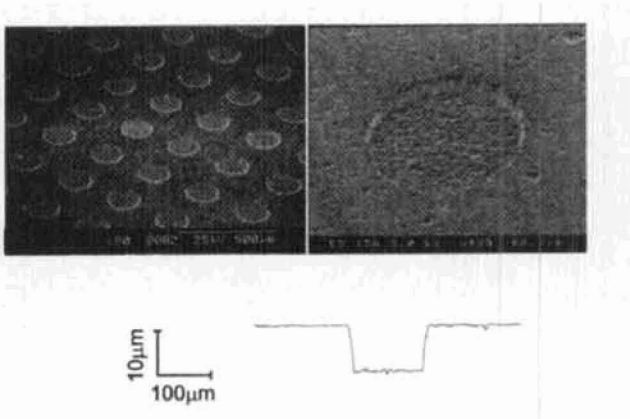

Fig. 2—The SEM photographs and cross profile of the micro-pit produced by IRE.

forming. The liquid trapped in the pits can be considered as a secondary source of lubricant, which is squeezed out or drawn by the relative movement to permeate into surrounding areas to reduce the friction and retard the galling (Anno, et al., (1969)).

However, analytical solutions are still difficult to yield true and exact results when dealing with texture lubrication. It is not only because the problem of free boundary associated with cavitation is so complicated that many assumptions are needed, but also, there is not enough theory to deal with the phenomenon happening in EHL and mixed lubrication regime. Especially for the ceramics of Si family sliding in water, so little is known about the properties of tribo-chemical products, that it is very difficult to simulate the lubrication conditions even without surface texture.

Therefore, the purpose of this research is to study the effects of micro-pits on the critical load for the transition from EHL to mixed lubrication in the cases of bearing type contact (with relatively rich water supply) and seal type contact (with relatively poor water supply), and to make an attempt to clarify the micro-pit lubrication mechanisms for SiC sliding in water.

EXPERIMENT

Specimens

Figure 1 shows the combinations of specimens used in this research. Both disk and cylinders were made of SiC sintered without pressurization. Its physical properties are listed in Table 1.

The sliding test was performed between the end faces of a cylinder [Fig. 1(a), outer and inner diameter are 20 and 10 mm respectively, thickness is 10 mm] and a disk [Fig. 1(b), diameter is 20 mm, thickness is 5 mm]. The bearing type contact uses a cylinder with two grooves (4×0.5mm) on the end face so as to be able to supply relatively sufficient water to the friction faces. The seal type contact uses a cylinder without groove so that the water supply is relatively insufficient compared to that of bearing type contact.

The end face of the disk was textured with micro-pits arranged in a square array as shown in Fig. 2 by the way of ion reaction etching (IRE). IRE is a widely used method for the process of MEMS and IC. It ionizes the reactive gas by electric discharge, then accelerates ions to make the target reacted and sputtered.

TABLE 2—GEOMETRICAL PARAMETERS OF THE DISKS

No.	Pit Diameter d (μm)	Pit Depth h (μm)	Pit Interval l (μm)	Pit Area Ratio r (%)
1	0	0	0	0
2	50	3.2	200	5.0
3	150	2.0 ~ 13.2	800 ~ 280	2.8 ~ 22.5
4	250	2.4 ~ 16.6	1330 ~ 470	2.8 ~ 22.5
5	350	3.2	1870 ~ 650	2.8 ~ 22.5
6	500	3.4	2670 ~ 930	2.8 ~ 22.5
7	650	3.3	2600	5.0

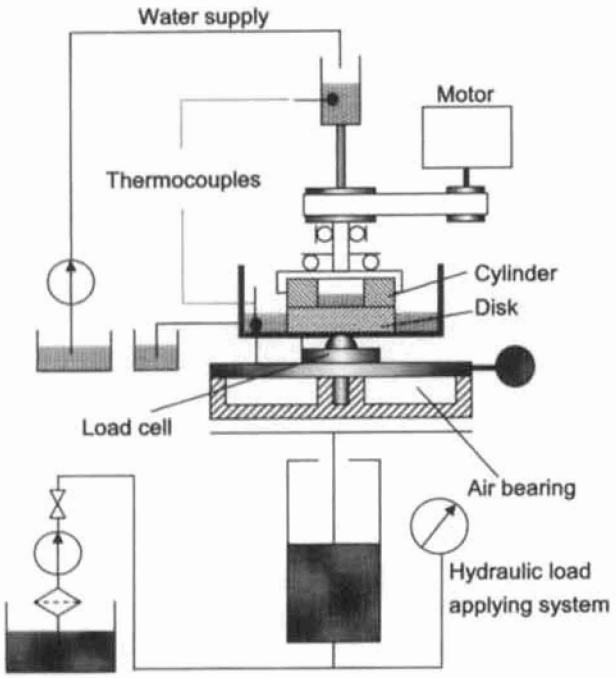

Fig. 3—Schematic diagrams of experimental apparatus.

Since the material is etched mainly in the direction of ion movement, the pits were formed in the shape of well as shown in Fig. 2. The round walls of the pits are near normal to the end face. The roughness of the pit bottom was related to the roughness of the original surface before etching and the anisotropic etching property of SiC material. The diameter and arrangement of the pits was determined by the metal mask formed on the surface. The depth of pits was controlled by etching time. The intervals between pits were changed to get a series of pit area ratios.

Table 2 shows the disks used in this study. They have the pit patterns with diameters ranging from 50 to 650 μm, depths from 2.0 to 16.6 μm, and pit area ratios from 0 to 22.5%.

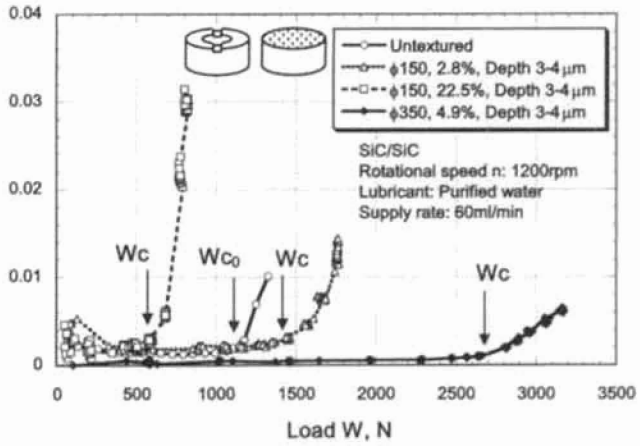

Fig. 4—Friction coefficient μ *vs.* load W for SiC cylinder/SiC disk in water at rotational speed of 1200 rpm.

Apparatus

Figure 3 shows the apparatus used in this experiment.

The cylinder is mated to the disk and driven by a motor with an adjustable rotational speed. The disk is supported by a half-spherical tip so that its friction surface is automatically aligned to match the surface of the cylinder. Load is applied by a hydraulic system from the bottom of the disk. Purified water is filled into the center hole of cylinder by a volume controllable pump. The temperature of the water before and after friction is monitored by thermocouples. Load and friction torque are detected by load cells. An air bearing is used to support the disk so that very small friction torque (<0.001Nm) can be detected accurately.

An auto-stop system is used to stop the load applying system and the driving motor to avoid the damage to apparatus and specimens when friction toque increases rapidly.

The temperature of the water supplied to the friction surfaces was accurately controlled to around 20°C since past studies showed that temperature has a large effect on the friction of SiC.

Bearing Type Experiments

Since the friction of SiC in water is very sensitive to the surface roughness, the same running-in process was carried out for all the specimens first. And then, friction coefficient was measured under certain rotational speed and load when friction became stable.

Figure 4 shows the typical trends of the friction coefficient for SiC sliding in water. The common feature of these curves is that the friction coefficient remains at a very low level (<0.005) while the load is light, and when the load exceeds a certain value, the friction suddenly rises. If the load was increased continually, seizure would occur although the value of friction coefficient is still low (<0.05) at that time.

It is clear that friction properties are obviously influenced by the surface texture. In this figure, the low friction ranges are expanded by the texture pattern with diameter of 150 μm, pit area ratio of 2.8% and the pattern with diameter of 350 μm, pit area ratio of 4.9%, but is reduced by the texture pattern with diameter

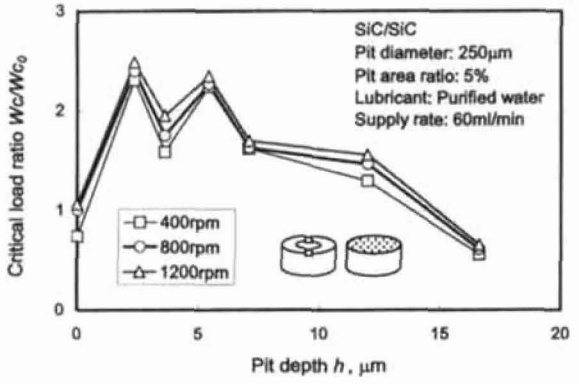

Fig. 5—The effect of the pit depth on the critical load ratio.

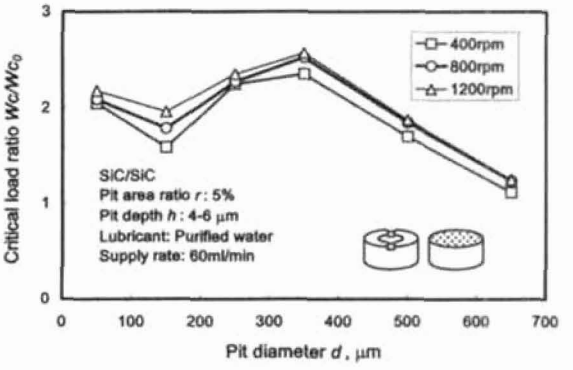

Fig. 7—The effect of the pit diameter on the critical load ratio.

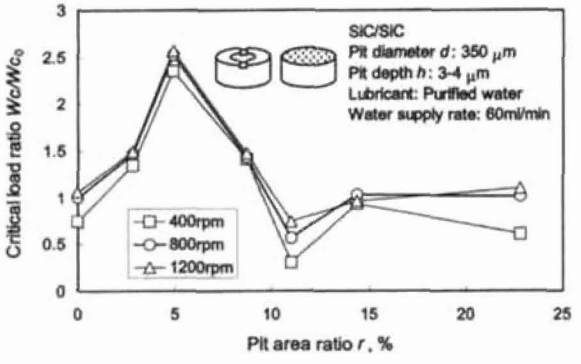

Fig. 6—The effect of the pit area ratio on the critical load ratio.

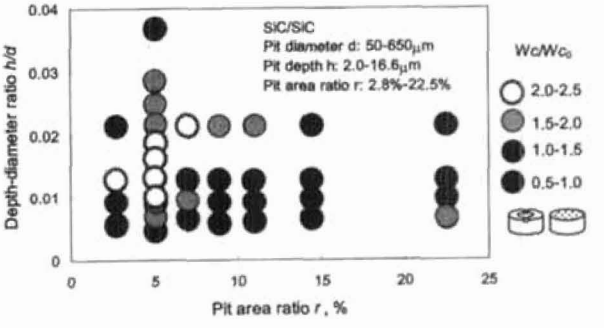

Fig. 8—The distribution of optimum pit pattern of SiC in bearing type contact sliding in water.

of 150 μm, pit area ratio of 22.5%. This indicates that there should exist some optimum patterns of micro-pits which could maximize the low friction range of SiC sliding in water, and too high pit area ratio increases the contact pressure which results in the increase of friction.

There is not enough positive proof to make sure the lubrication regime falls into the low friction ranges shown in Fig. 4. The fact that the low friction range exists and its value is very low, approximately 0.001-0.003, suggests it was in the regime of hydrodynamic lubrication or elastic hydrodynamic lubrication. Thus, the start of the rapid increase of friction coefficient from a stable low value can be considered as the transition of the lubrication regime from hydrodynamic to mixed and above.

Therefore, the load, at which the friction coefficient starts its sudden increase (Fig. 4), was defined as the critical load Wc for the transition of the lubrication regime from hydrodynamic to mixed so as to evaluate the effect of the surface texture in this experiment. A high critical load means the hydrodynamic lubrication region is large, and the load carrying capacity is great.

Figures 5 through 7 are examples of the representative effects of the pit depth, pit area ratio and pit diameter on the critical load Wc. They were summarized from the results of basic friction test such as previously shown in Fig. 4. In order to show the effect of surface texture clearly, the Y axis of these graphs were drawn in the form of critical load ratio Wc/Wc_0, where Wc stands for the critical load of textured specimen, and Wc_0 for the critical load of untextured specimen at a rotational speed of 800 rpm.

The three curves in each graph were obtained at three different rotational speeds; 400, 800 and 1200 rpm. Generally, a higher rotational speed leads to a greater critical load although the difference is not very large.

It is found that all the parameters of pit depth, pit area ratio and diameter have obvious effect on the critical load Wc, and they have their optimum range, respectively. These results remind us that the effects of the pit depth, diameter and the pit area ratio should be considered comprehensively for the purpose of maximizing the critical load. In other words, the way to demonstrate the optimum combinations of pit geometry and distribution is needed.

Figure 8 is an attempt to summarize the effects of the pit depth, diameter and pit area ratio into one graph. The vertical axis indicates the geometrical factor of pit, the depth-diameter ratio h/d, and the horizontal axis indicates the pit distribution factor, the pit area ratio r. The conditions marked as "○" are these at which the

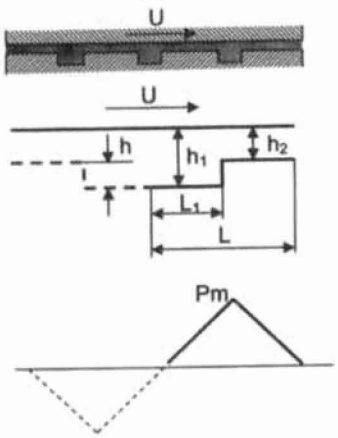

Fig. 9—The pit geometry.

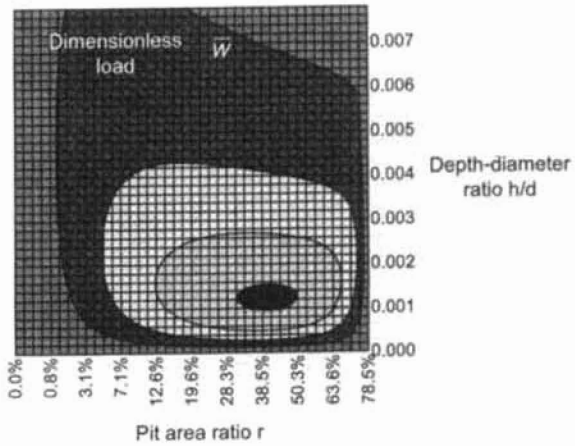

Fig. 10—Theoretical effect of pit area ratio r and depth-diameter meter ratio h/d on the dimensionless load.

critical load was increased to at least two times greater than that of an untextured one, "◍", "●" represent the increment between 1.5~2.0 times, 1.0~1.5 times respectively, and "●" represents that critical load was decreased at that condition. It is now clear that there exists a large region around the pit area ratio of 5% and depth-diameter ratio of 0.015, where critical load was increased to at least two times greater than that of an untextured one.

Simplified Theoretical Analysis

A theoretical analysis was performed to evaluate the hydrodynamic pressure generated by micro-pit. Because of the complexity of the free boundary problem associated with cavities, as well as the interaction between pits, several assumptions were made, and the results of the theoretical analysis are expected to show only the trends of the effects of the pit depth, diameter and the pit area ratio.

The problem has been simplified to two dimensions as shown in Fig. 9. Each pit is assumed to be antisymmetric, that is, the pressure increases on one side while decreases on the opposite side. Since cavities are proved to be generated when the pressure decreases lower than cavitation pressure, the pressure of the negative side is replaced by the cavitation pressure, which was simplified to 0 in this study. Therefore, only the side with positive pressure, which could be considered as a step bearing, needs to be calculated. Additionally, the pressure at the midpoint between the two pits was also assumed to be 0. It means a short interval between pits would result in a rapid decrease of the hydrodynamic pressure.

The pressure distribution along a step bearing resembles a triangle as shown in Fig. 9. The maximum pressure occurs at the step, which is given by:

$$pm = \frac{6\eta UL}{h_2^2} \cdot \frac{s(1-s)(a-1)}{a^3(1-s)+s}$$

where $a=h_1/h_2$, $s=L_1/L$.

Therefore, the total load in two dimensions, which can be supported by this pit, is given by:

$$W = L\frac{P_m}{2} = \frac{3\eta UL^2}{h_2^2} \cdot \frac{s(1-s)(a-1)}{a^3(1-s)+s}$$

which includes two main parts, the left part are those which include operating conditions (η, U) and given conditions (h_2, L), the right part are the conditions which vary only according to the geometry and distribution of micro-pits. Therefore, the right part is defined as a dimensionless load to show the effects of the pit geometry and distribution as shown below.

$$\bar{W} = \frac{s(1-s)(a-1)}{a^3(1-s)+s}$$

In order to compare the results between the theoretical analysis and experiments, the dimensionless load was calculated and plotted on Fig. 10 with the same x and y axis as on Fig. 8.

It is clear that the results of the theoretical analysis present a similar trend to the experimental data obtained in bearing type contact. This indicates that the hydrodynamic effect acts as the leading role in the micro-pits lubrication under the condition of bearing type contact, and the existence of optimum geometry and distribution range for the critical load is reasonable.

For the optimum geometry and distribution values of micro-pits, there are large differences between the results of experiment and calculation. The theoretical value of the pit area ratio to generate highest hydrodynamic pressure is near 40%, while experiment results indicate the optimum value is around 5%. This might be due to that in experiment, critical load is the index to show overall load carrying capacity of the contact, although the pit area ratio as high as 40% generates highest hydrodynamic pressure, it also gives a negative effect, that is, a reduction of the contact area which results in the increase of contact pressure. For the difference of the depth-diameter ratio between calculation and experiment, experimental results indicate that the pit deeper than the theoretical value results in a higher critical load.

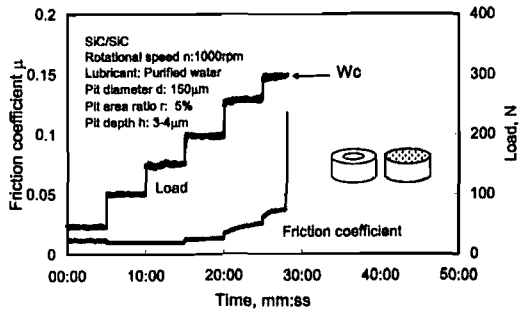

Fig. 11—The friction properties of SiC in seal type contact sliding in water.

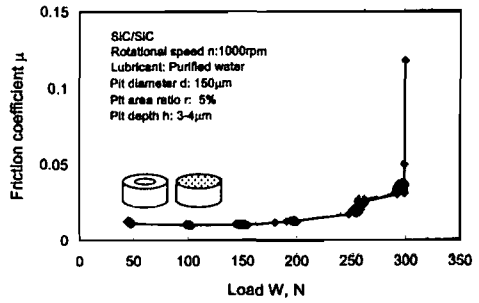

Fig. 12—The friction coefficient μ *vs.* load W for SiC in seal type contact sliding in water.

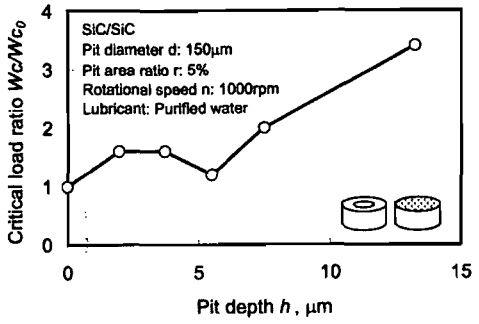

Fig. 13—The effect of pit depth in the case of seal type contact.

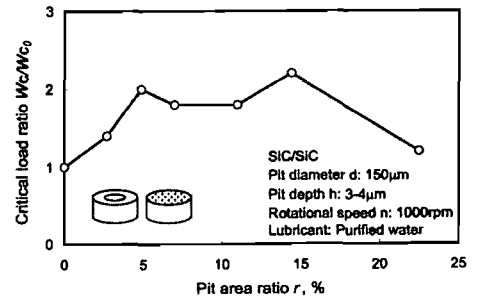

Fig. 14—The effect of pit area ratio in the case of seal type contact.

Seal Type Experiments

The textured disks tested in the experiment of bearing type contact were then used to slide against the cylinder without groove to simulate the condition of mechanical seals.

Figure 11 shows the variation of friction coefficient while load was increased. In the case of this contact, the increase of friction had not a quick response to the increase of load. For example, the friction got rapid increase after the load of 300N was applied for several minutes in this figure. From Fig. 12, it was found that the relationship between friction coefficient and load shows similar trend to that of bearing type contact, that is, there is a low friction range and friction increases rapidly after load exceed a certain value.

Therefore, the same method as the experiment of bearing type contact was used to evaluate the pit effect in the case of seal type contact. That is, first to get the critical load Wc for the transition of the lubrication regime from hydrodynamic to mixed, then, to calculate the critical load ratio Wc/Wc_0 through the comparison of critical load between the textured and untextured.

Figures 13 through 15 are representative figures which show the effect of the pit diameter, pit area ratio and pit depth on the critical load ratio Wc/Wc_0. The curves show some differences compared to those obtained in the case of bearing type contact.

As the same way to that of bearing type contact, the experimental results of the effect of the pit diameter from 50 ~ 650 μm, pit area ratio from 2.8 ~ 22.5% and pit depth from 2.0 ~ 16.6 μm were summarized to Fig. 16, whose vertical axis indicates the geometrical factor of pit, the depth-diameter ratio h/d, and the horizontal axis indicates the pit distribution factor, the pit area ratio r. Compared with Fig. 8, there is not any clear concentrated optimum region of pit pattern as shown in Fig. 8, which is supposed to be preferable for the generation of hydrodynamic pressure. Furthermore, the conditions marked as "❂," which make at least two times increment of critical load over untextured one, shift to the up-right direction in this figure. This means the texture pattern with greater area ratio and deeper depth is better to get greater critical load ratio. It implies that in the case of seal type contact, the water storage ability of micro-pits becomes more important than the ability to generate hydrodynamic pressure. The reason is probably that the water stored is helpful to the tribo-chemical reaction, which is necessary for the low friction in the case of SiC sliding in water.

Since only relative increment ratio of critical load are displayed in Fig. 8 and Fig. 16, it is also important to compare the absolute value of the critical load in these two cases. Figure 17 is an example which shows the effect of pit area ratio on the critical load Wc in the cases of bearing type contact and seal type contact. First of all, the effect of grooves is great. With relative sufficient supply of water, even without micro-pit, the critical load is much greater than that without grooves. Second, the pit pattern with pit area ratio of 7% increased the critical load with the increment of about 1200N in bearing type contact, which is more than two

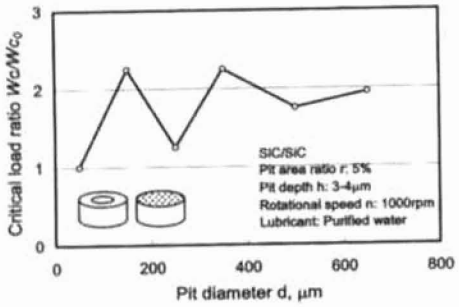

Fig. 15—The effect of pit diameter in the case of seal type contact.

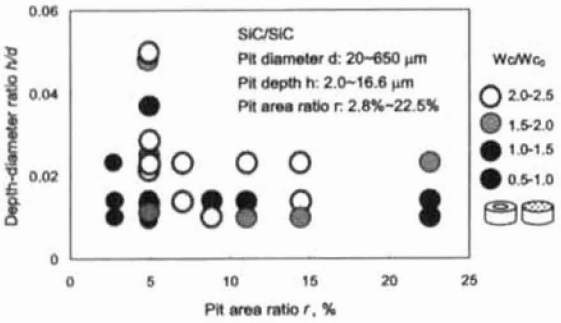

Fig. 16—The distribution of optimum pit pattern of SiC in seal type contact sliding in water.

times of that of untextured one. Meanwhile, in the case without groove, micro-pits in the case of seal type contact also made the increment about two times that of the untextured one, and the importance is that it was realized within a wider pit area ratio range from 4.9% to 14.4% although the absolute increment is small.

As mentioned above, in the case of bearing type contact, the main micro-pit effect is the generation of hydrodynamic pressure. It is reasonable that the grooves on the contact surface supply necessary water to enable this function of micro-pits. The absolute increment far exceeds that in the case of seal type contact.

For the seal type contact, it is found that the increment about two times of that of untextured disk can be obtained within the pit area ratio range from 4.9 to 14.4%. It is also reasonable that water supplied to the contact surface is not enough to generate hydrodynamic pressure, so the ability for preserving enough water to maintain tribo-chemical reaction becomes dominant.

Based on the experimental results and discussion above, the authors may explain the mechanism of Fig. 17 as shown in Fig. 18.

CONCLUSIONS

Micro-pits were formed on the contact surface of SiC to improve its load carrying capacity or anti-seizure ability in water. The experiments in bearing type contact and seal type contact were carried out, and the pit effect on the critical load for the transition from hydrodynamic to mixed lubrication regime were studied experimentally. The mechanism of micro-pit lubrication was discussed through comparing the pit effect in the cases of different contact type. The following conclusions have been drawn as the most significant:

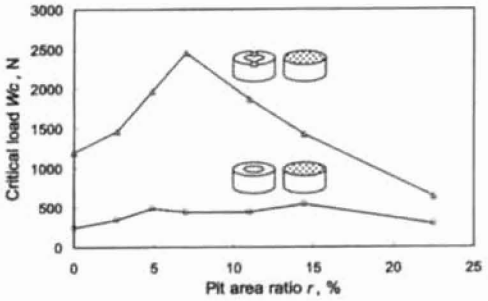

Fig. 17—A comparison of the micro-pit effect in the cases of bearing and seal type contact.

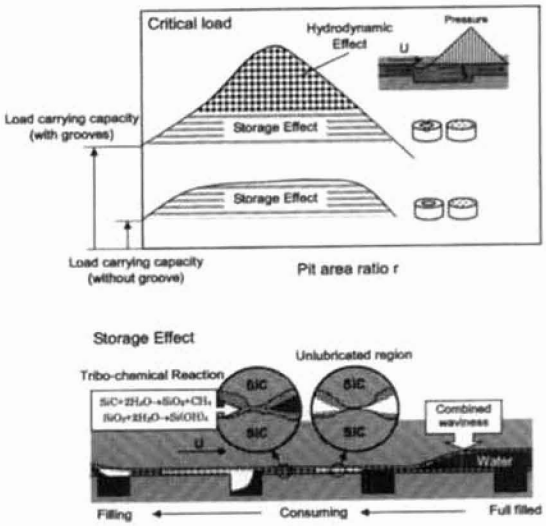

Fig. 18—A supposition to the micro-pit lubrication mechanism in the contact of bearing and seal type.

1. Both in the case of bearing type contact and seal type contact, micro-pit texturing is an effective way to increase the critical load. The optimum pit conditions, which are able to increase the critical load at least two times greater than that of untextured one, was obtained in the case of bearing type contact and seal type contact respectively.
2. In the case of bearing type contact, the optimum conditions of micro-pits concentrated in the region around the pit area ratio r of 5%, and depth-diameter ratio h/d of 0.015.
3. In the case of seal type contact, the optimum conditions did not concentrate as that of bearing type contact. It was found that the pit patterns, which have greater pit area ratio and higher depth-diameter ratio than those in bearing type contact, would give a large improvement in the critical load.

REFERENCES

(1) Anno, J. N., Walowit, J. A. and Allen, C. M. (1968), "Microasperity Lubrication," *Jour. of Lubr. Tech.*, **4**, pp 351-355.

(2) Anno, J. N., Walowit, J. A. and Allen, C. M. (1969), "Load Support and Leakage from Microasperity-Lubricated Face Seal," *Trans. ASME, Jour. of Lubr. Tech.*, pp 726-731.

(3) Etsion, I. and Burstein, L. (1996), "A Model for Mechanical Seals with Regular Micro Surface Structure," *Trib. Trans.*, **139**, 3, pp 677-683.

(4) Etsion, I., Kligerman, Y. and Halperin, G. (1999), "Analytical and Experimental Investigation of Laser-Textured Mechanical Seal Faces," *Trib. Trans.*, **42**, 3 pp 511-516.

(5) Geiger, M., Roth, S. and Becker, W. (1998), "Influence of Laser-Produced Microstructures on the Tribological Behaviour of Ceramics," *Surface and Coatings Tech.*, **101**, 1-3, pp 17-22.

(6) Halperin, G., Greenberg, Y. and Etsion, I. (1997), "Increasing Mechanical Seal Life with Laser-Textured Seal Faces," in *Proc. of the 15th Int. Conf. on Fluid Sealing BHR Group, Maastricht*, pp 3-11.

(7) Hamilton, D. B., Walowit, J. A. and Allen, C. M. (1966) "A Theory of Lubrication by Micro-Irregularities," *Trans. ASME, Jour. of Basic Engineering*, **88**, 1, pp 177-185.

(8) Ishigaki, H., Nagata, R. and Iwasa, M. (1988), "Effect of Absorbed Water on Friction of Hot-Pressed Silicon Nitride and Silicon Carbide at Low Speed Sliding," *Wear*, **121**, pp 107-116..

(9) Lebeck, A. O. (1987), "Parallel Sliding Load Support in the Mixed Friction Regime, Part 2-Evaluation of the Mechanisms," *Trans. ASME, Jour. of Trib.*, **109**, 1, pp 196-205.

(10) Lo, S. W. and Horng, T. C. (1999), "Lubricant Permeation from Micro Oil Pits under Intimate Contact Condition," *Trans. ASME, Jour. of Trib.*, **121**, pp 633-638.

(11) Ludwig, L. P. and Greiner, H. F. (1978), "Designing Mechanical Face Seals for Improved Performance Part 2 – Lubrication," *Mechanical Engineering*, **100**, 12, pp 18-23.

(12) Nau, B. S. (1997), "Mechanical Seal Face Materials," in *Proc. Instn. Mech. Engrs.*, **211**, J, pp 165-183.

(13) Sugita, T., Ueda, K. and Kanemura, Y. (1984), "Material Removal Mechanism of Silicon Nitride During Rubbing in Water," *Wear*, **97**, pp 1-8.

(14) Tejima, Y., Ishiyama, S. and Ura, A. (1999), "The Influence of Pores at Sliding Faces and the Pores Diameter on Mechanical Seals Performance," *Jour. of Japanese Society of Tribologists*, **44**, 6, pp 54-61.

(15) Tom, L. (1994), "Development of Non-Contacting, Non-Leaking Spiral Groove Liquid Face Seals," *Lubr. Eng.*, pp 625-631.

(16) Wang, X., Adachi, K, Kato, K. and Aizawa, K. (2000), "The Effect of Surface Texture on Seizure between SiC Cylinders Sliding in Water," in *Proc. of the Int. Trib. Conf., Nagasaki*, pp 869-874.

(17) Wang, X., Kato, K., Adachi, K. and Aizawa, K. (2001), "The Effect of Laser Texturing of SiC Surface on the Critical Load for the Transition of Water Lubrication Mode from Hydrodynamic to Mixed," *Trib. Int.*, **34**, 10, pp 703-711.

(18) Wang, X. and Kato, K. (2002), "Micro-Pit Effect on Anti-Seizure Ability of SiC Seal in Water," in *Proc. of 13th Int. Colloquium Trib., Stuttgart*, pp 2243-2248.

(19) Wong, H. C., Umehara, N. and Kato, K. (1998), "Frictional Characteristics of Ceramics under Water-lubricated Conditions," *Trib. Letters*, **5**, 4, pp 303-308.